J Ther Eng, Vol. 8, No. 5, pp. 632–641, September 2022

Journal of Thermal Engineering
Web page info: https://jten.yildiz.edu.tr
DOI: 10.18186/thermal.1190529

Journal of Thermal Engineering

Research Article

Numerical analysis of an isolation room to prevent the spread of COVID-19

Erhan ARSLAN[1,*]

[1]*TUBITAK Marmara Research Center, Kocaeli, Türkiye, 41310*

ARTICLE INFO

Article history
Received: 27 May 2021
Accepted: 20 August 2021

Keywords:
CFD; Isolation Room; Numerical Analysis; COVID-19

ABSTRACT

COVID-19 virus, which is a member of the coronavirus family, is a virulent virus that is transmitted by physical contact or air and results in death in infected people. People infected by the COVID-19 virus must be kept in quarantine in a closed area. Therefore, it is very important for the health of the individuals (patient, doctor, nurse, etc.) in the isolation room that, where the area kept closed is completely free of virus. This study was conducted to examine the flow dynamics of the air in the isolation chamber. With the simultaneous operation of the sanitized air machine and the ventilation in the room, it is aimed to investigate the virus killing effect of the air mixed with each other. The flow dynamics, velocity, temperature and turbulence kinetic energy of the air in the isolation chamber were examined. Investigations were carried out to ensure that the mixture of the two air in the room was better and distributed throughout the room.

Cite this article as: Arslan E. Numerical analysis of an isolation room to prevent the spread of COVID-19. J Ther Eng 2022;8(5):632–641.

INTRODUCTION

The coronavirus (COVID 19) disease, which is thought to have emerged in Wuhan, China at the end of 2019 and spread all over the world in a short time, has become an important epidemic that continues to threaten the whole world. Which affected nearly 6 million people and almost 300,000 deaths, Severe Acute Respiratory Syndrome coronavirus 2 (SARS-CoV-2) or only Covidien-19 (COVID-19) with a terrible time, it has emerged as a global pandemic and rising quickly [1].

This disease is transmitted by sneezing as well as by coughing or even inhalation of droplet nuclei (Φ <5μm) produced during speech or by contact. Exhaled droplets from the COVID-19 patient or the active carrier of the virus may accumulate in the mucous membrane of the conjunctiva of the mouth, nose or eyes of other people in close contact. The virus is transmitted through personal contact with a COVID-19 patient or from utensils, furniture, surfaces, etc. It can be transmitted through indirect contact

***Corresponding author.**
*E-mail address: erhana1985@gmail.com, erhan.arslan@tubitak.gov.tr

This paper was recommended for publication in revised form by Regional Editor Erman ASLAN

Published by Yıldız Technical University Press, İstanbul, Turkey

with fomites. Usually, symptoms such as fever, shortness of breath, sore throat, and cough appear in infected people [2]. The disease causes respiratory diseases such as pneumonia and acute respiratory distress syndrome, resulting in rapid death depending on the age, lung condition, immunity and sociodemographic profile of those affected. Many studies [3–5] have shown that this virus is highly harmful. It has become a pandemic reported by the World Health Organization (WHO) (characterizes COVID). Droplets generate aerosol by coughing, sneezing or speaking. Virus-containing droplets form the substrate for viruses in the isolated area for airborne transmission of this disease. In addition, environmental conditions (relative humidity, temperature, precipitation, etc.) are specified as effective parameters for the virus [6–8].

Removal of airborne particles in airborne infection isolation rooms is important for the infection control of airborne diseases. Keeping COVID 19 patients and those with symptoms in isolated rooms is essential to prevent the disease. These isolated rooms are called Airborne Infection Isolation Rooms (AII). The virus can be carried in the air released from these rooms. An effective strategy must be implemented to prevent this [9,10]. In a study in which air and surface samples were tested to determine the distribution of severe acute respiratory syndrome coronavirus in hospital wards in Wuhan, China, it was stated that contamination in intensive care units was higher than in general services. A study was conducted at a shopping mall in Wenzhou, China, to determine possible modes of virus transmission. The study, which investigated a number of several COVID-19 cases, showed that the indirect transmission of the virus was likely caused by the virus transmission of common objects, aerosolization of the virus in a confined space, or the spread from asymptomatically infected people [11]. Various methods have been used in the disinfection of the exhaust gas. HEPA filtration, sanitization, heating UV are among the common examples [12–16].

Since the heating, ventilation and air conditioning (HVAC) system plays a very important role in the transmission of SARS-CoV-2, it has been a problem for this industry that the HVAC systems will be operated at maximum efficiency. The task of HVAC systems is to provide a healthy and comfortable environment. However, it has been found that insufficient ventilation in confined spaces is associated with an increase in respiratory tract infections [9,17,18]

Few studies have been conducted to examine the effects on the design and of isolation rooms [18,19].

Thermal cabinet design using different approaches has been studied by many researchers [20–23]. Computational fluid dynamics (CFD) is of great importance as it provides information in the thermal and airflow fields. Many studies [23–26] have been done to track the motion of suspended particles. In addition, Yadav et al. [27] suggested in his study that the results obtained from the 2-dimensional model are close to the real results as analysed with the 3-D flow. The CFD analysis can be used to determine the trajectory of these particles, determine their velocity and motion, and variables such as dynamic processes. It is important to investigate the sterilization of isolation rooms in hospitals, as there is a high risk of airborne transmission of the COVID-19 virus. Sterilization of the limited volume of air in the room is very important for healthcare professionals. The aerosolizing sanitization process of air can be designed by the CFD. However, there are a limited number of reports on the subject in the literature.

This study focuses on the distribution of air released from sanitized air and ventilation within the room. It is intended to demonstrate how the flow behaves to achieve complete sanitation to ensure that the air released into every corner of the isolation room kills the COVID-19 virus. The data of the study were compared with a previous experimental study [28] to provide validation. The main purpose of the study is to examine both the ventilation and the flow physics of the air coming out of the sanitization machine to kill the COVID virus in the isolation room. In this context, the flow physics will be utilized to eliminate or minimize the virus in the isolation room, which is examined numerically.

COMPUTATIONAL DESIGN AND METHODOLOGY

Geometrical Design

Fig. 1 shows the model of the isolation room whose dimensions are taken from a hospital. All of the structures required in the isolation room (patient bed, door, ventilation, sanitized air machine) are shown in the model with their original dimensions. The length, width, and height

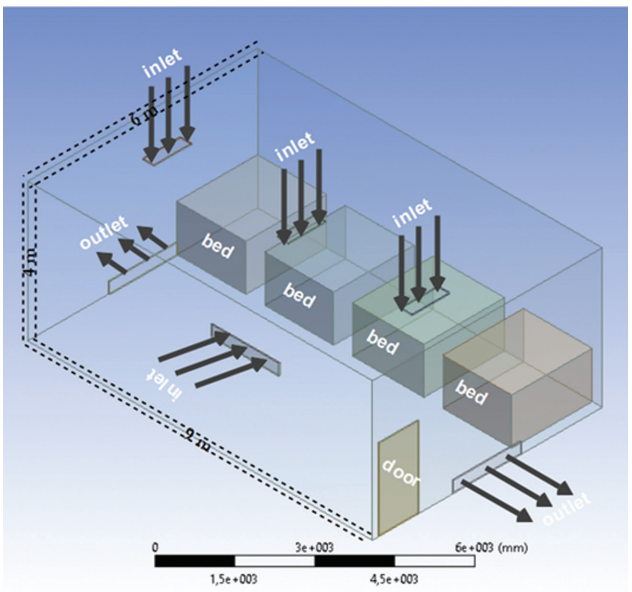

Figure 1. Schematic diagram of the computational domain (isolation room of hospital).

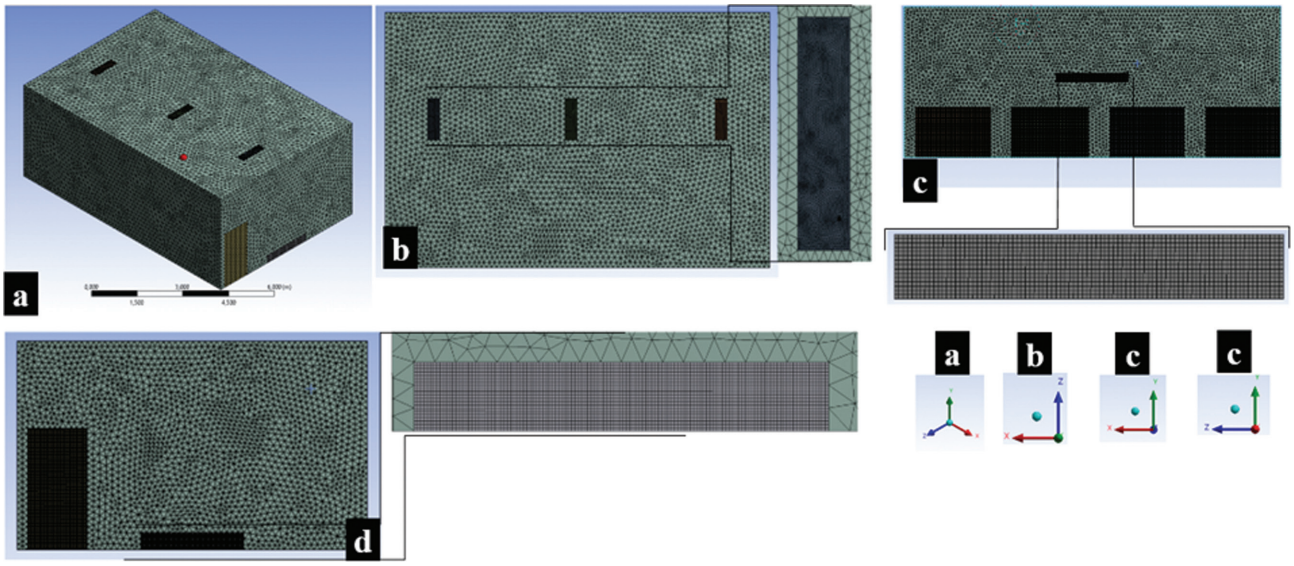

Figure 2. The geometry of mesh structure. (a) Isometric, (b) X-Z cross section, (c) X-Y cross section, (d) Y-Z cross section.

of the isolation room are 9.1, 6.1, and 3.7 m respectively. The length and width of the ventilation grid are 1 and 0.3m respectively. The grill of the sanitized air machine where the air is blown is 1.8 and 0.3m. The exhaust air grids are also 1.8 and 0.3m.

Mesh Structure

The mesh structure is defined as the ratio of the number of elements of the geometric structure to the number of nodes. More results that are accurate are obtained with an increasing number of elements. Decreasing the number of elements or nodes can lead to wrong results. The mesh structure is very important such studies. The correct mesh ratio is vital in optimizing results [29,30]. The mesh structure of the study is shown in Fig. 2.

Discretization is required to solve partial differential equations which include the governing (Continuity Eq. 1, Momentum Eq. 2-3 and Energy Eq. 4) equations [31,32]. Second-order upwind schema with Boussinesq approximation is used for discretization. Simulation of the unstable air provides information about the flow physics of the system (i.e. the isolation room). The process of purifying the air in the isolation chamber by diffusion reveals the necessity of the simulation event to better understand the flow physics. It also includes phenomena such as pressure forces, buoyancy, forced convection, and heat transfer. The simulation of the natural ventilation process of the isolation chamber provides information about the behavior of flow physics [19].

Continuity equation [33,34]

$$\frac{\partial \rho}{\partial t} + \nabla(\rho v) = 0 \qquad (1)$$

Momentum equations [33,34]

$$\frac{\partial(\rho u)}{\partial t} + \nabla(\rho u V) = -\frac{\partial p}{\partial x} + \mu\nabla(\nabla u) + \rho g x \qquad (2)$$

$$\frac{\partial(\rho v)}{\partial t} + \nabla(\rho v V) = -\frac{\partial p}{\partial x} + \mu\nabla(\nabla v) + \rho g y \qquad (3)$$

Energy equation [33,34]

$$\rho c_p\left(\frac{dT}{dt} + \nabla T V\right) = \nabla(\nabla k T) \qquad (4)$$

Standard k-epsilon Model

To numerically model laminar transitional flows, the transition Standard k - ε model is used in the present study. The k-ε model contains many unknown terms. In order to provide a more practical approach, this model should be applied to many models with turbulence. This situation reduces the unknowns. The standard k- ε model used as a publication is defined as two equations (Eq. 5 - 7). k denotes turbulent kinetic energy (Eq. 5, 6) and ε turbulent propagation (Eq. 7) [33].

$$\frac{\partial(\rho k)}{\partial t} + \frac{\partial(\partial k u_i)}{\partial x_i} = \frac{\partial}{\partial x_j}\left[\frac{\mu_t}{\sigma_k}\frac{\partial k}{\partial x_j}\right] + 2\,\mu_t E_{ij} E_{ij} - \rho \qquad (5)$$

$$\frac{\partial(\rho k)}{\partial t} + \frac{\partial}{\partial x_j}(\rho U_j k) = \frac{\partial}{\partial x_j}\left[\left(\mu + \frac{\mu_\tau}{\sigma_\kappa}\right)\frac{\partial k}{\partial x_j}\right] + P - \rho\varepsilon + P_{kb} \qquad (6)$$

Turbulent dissipation rate ε,

$$\frac{\partial(\rho\varepsilon)}{\partial t}+\frac{\partial(\partial\varepsilon u_i)}{\partial x_i}=\frac{\partial}{\partial x_j}\left[\frac{\mu_t}{\sigma_\varepsilon}\frac{\partial\varepsilon}{\partial x_j}\right]+C_{1\varepsilon}\frac{\varepsilon}{k}2\mu_t E_{ij}E_{ij} - C_{2\varepsilon}\rho\frac{\varepsilon^2}{k} \quad (7)$$

It is assumed that the turbulent viscosity (□t) is proportional to the turbulence velocity and the length scale. These scales are derived from turbulence kinetic energy (k) and propagation rate (ε). Turbulent viscosity expression is as follows (Eq. 8) [35].

$$\mu_t=\rho C_\mu\frac{k^2}{\varepsilon} \quad (8)$$

C_μ is an experimental constant. In the k-ε turbulence model, k and ε values are needed to calculate the turbulent viscosity (□t). These values are obtained from the Eq. 5–7 [36,37]. The turbulence kinetic energy generation due to mean velocity gradient and viscous forces, experimental constants $C_{\varepsilon 1}$ and $C_{\varepsilon 2}$, and σ_ε, σ_κ Prandtl numbers. The values of the constants required for the solution are given in Table 1 [33]:

As in many approaches, there are negligence assumptions in this model as well. Consequently, the modelled ε transport model can be used in a very similar form to the k transport equation.

Validation of the Current Study and Mesh Independency

In this study, the flow physics in the isolation room was examined numerically. A comparison was made with a previous experimental study to prove the accuracy of the study. The velocities in the cases in the experimental study [28] (v = 1.36 and 0.68 m/s) were examined and compared with the speeds in this study. The measurement points in the experimental study were used as a basis for comparison.

Figure 3 (a) shows the measurement points, calculation area and velocity from various parts of the designed isolation chamber. It can be easily understood from Figures 3 (b) and (c) that the experimental [28] and current numerical values have a very good agreement against published data.

Mesh Independency

Mesh structure and independency analysis is an important issue for numerical studies to determine the optimum values of the study. In this context, combinations with different mesh numbers have been tried to determine the mesh structure of the isolation chamber. More results that are accurate were obtained compared to the increase in the number of meshes. However, as the number of meshes increased, temperature gives different results. The values obtained from the measurement point (P2) according to the number of meshes made for this study are shown in Fig 4. The error rate at low mesh counts (2042 and 5546) was measured as 19.2% and 13.2%. In other, mesh numbers of 24906, 33048, 44988, 65958, and 148949 these error rates were calculated as 8%, 7.2%, 0.4%, 4.8%, 4.4%, respectively. As can be understood from the error rates, the optimum mesh number for the study was obtained as 44988. The maximum and average skewness values in this mesh number were 0.84 and 0.15, respectively.

Table 1. Constants used in the k-ε model [25]

$C_{\varepsilon 1}$	$C_{\varepsilon 2}$	C_μ	σ_ε	σ_κ
1.44	1.92	0.09	1.3	1.0

RESULTS AND DISCUSSION

The CFD approach can be used to study the working fluid (air) in the comfort zone and the pollutants in the fluid [38]. Figs. 5 and 6 show the operating and non-working states of the sanitized air machine, respectively. The streamlines obtained only emerging from the operation of the sanitized air machine are given in Fig 5. Figs. 5a and 5b express top view (XZ plane) and 3D view (XYZ plane), respectively. According to the velocity distribution of the flow lines in the room, it was observed that the fresh air coming out of the sanitized air machine was distributed throughout the isolation room. The situation when the sanitized air machine is not working (Fig. 6) shows the setup of different isometric views of the isolation room. The top view of the continuously variable streamlines (XZ plane) is given in Fig. 6a. It is clear that the behavior of the fluid in the room is due to the ventilation gap positioned at the top. The 3-dimensional (XYZ plane) view of the room is given in Fig. 6b. As can be understood from here, it seems that the streamlines fall down the ventilation hole and hit the floor. It is clear that the fluid hitting the floor recoils and spreads to other parts of the room (walls, patient beds, etc.). Fig. 6 shows the streamlines in the room when only operating ventilation. It can be said that the current lines are distributed in the same density throughout the room. The figures below provide a quantitative review for the analysis of the flow, fluid velocity, and temperature and turbulence kinetic energy in the isolation room when the sanitized air machine and ventilation are operating simultaneously.

The velocity vector projection is shown in Fig. 7. This means that the longer vectors are faster. It can be said that the speeds slow down because of the encounter of the air coming from the horizontal (air coming from the sanitized air machine) and from the vertical ventilation direction. It is also seen that the air hitting the walls relatively slows down. Fig. 7 shows the velocity distributions of the air in the XY (Fig. 7a) and YZ (Fig. 7b) planes, respectively. In the case where the sanitized air machine and the ventilation

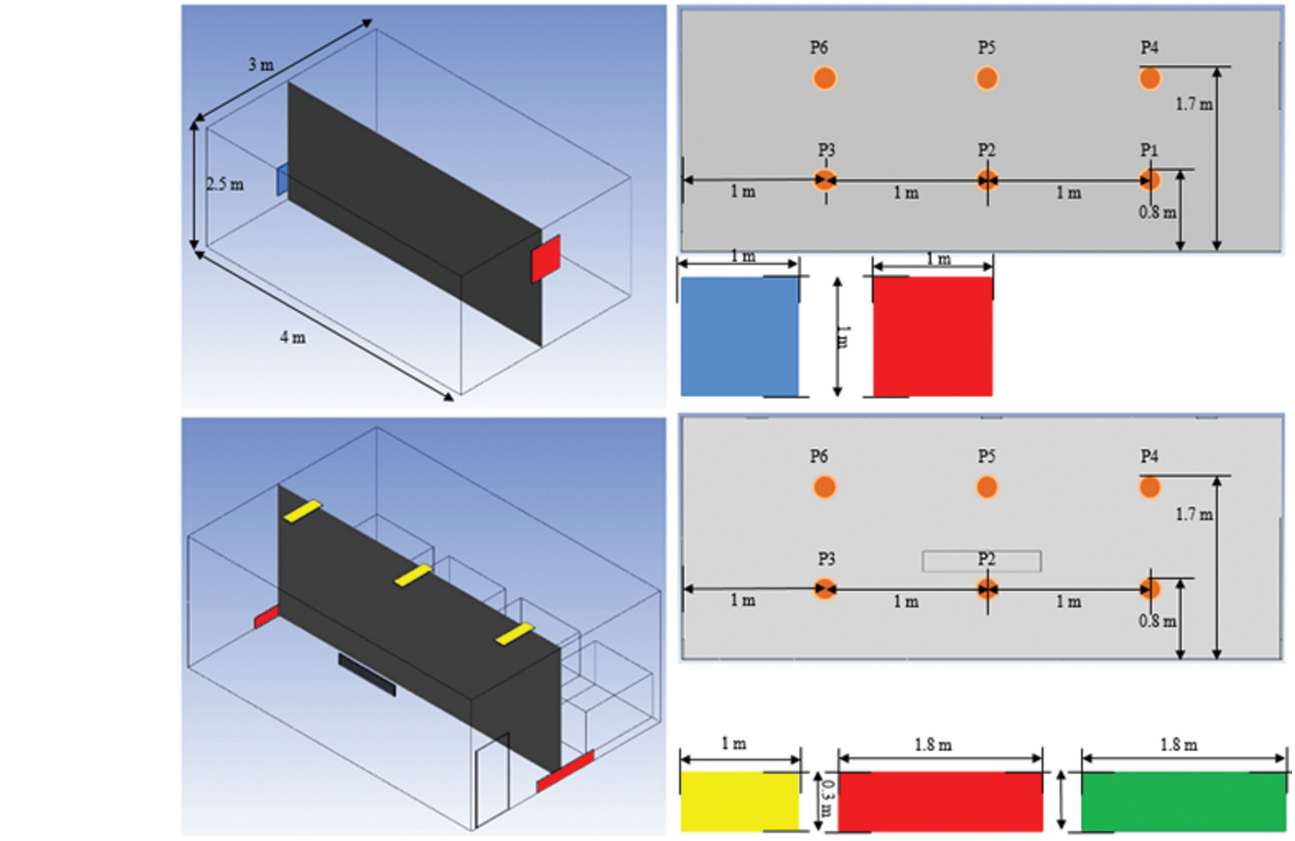

Figure 3. Validation of case. (a) Validation of measurement points by experimental study [28], (b) velocity =1.36 m/s and case C2 considered, (c) velocity = 0.68 m/s and case D1 considered.

are working together, it is seen that the inlet velocities are high in the XY plane, but the velocity approaches zero in the eddies. In the YZ plane, it can be seen from the way that eddies are formed by the collision of the two air.

Because of this mixing, the room is expected to be sterilized. This situation is very important for those staying in the isolation room.

Figs. 8a and 8b shows the temperature distributions when the sanitized air machine and the ventilation work together in the XY and YZ planes, respectively. Fig. 8a, showsthat inlet air and near the inlet contour was relatively lower than the ambient air temperature, while the temperature of the air leaving the sanitized air machine was higher. Accordingly, it is seen that the relatively cold

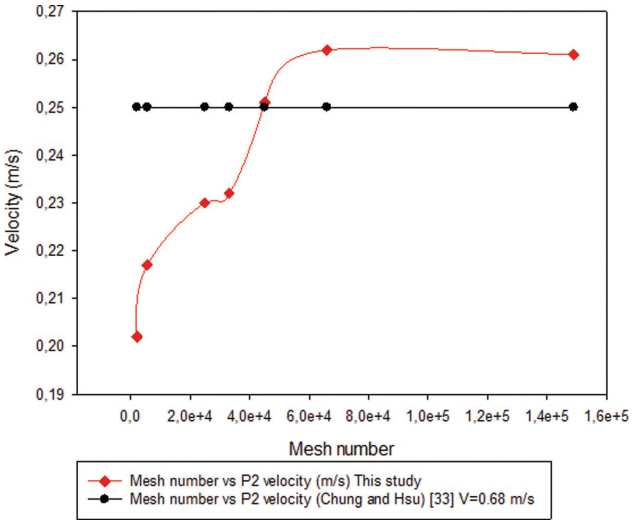

Figure 4. Mesh independence results for an isolation room.

air (24°C) coming from the ventilation is mixed with the warm air (30°C) from the sanitized air machine. In both cases (Figure 8a and b), the temperature gradient, which is the mixture of cold air coming from the ventilation and hot air coming from the sanitized air machine, creates asymmetrical contours. It is clear that in the section where the sanitized air machine is located, a better mix is observed in Figure 8b (right side).

The change of turbulent kinetic energy created by two airs mixed with each other in the room is given in Fig. 9. The representation of the region where the eddies are formed is shown in Figure 10b. Two large eddies are seen in Fig. 10b shown to identify regions of high turbulence. The density of turbulence is proportional to the density of the mixture [19,38]. This means that a better mixture is created due to high turbulence. Thanks to the mixture, the COVID-19 virus in the room will be completely destroyed. Thus, the lives of those staying in the room can be better protected.

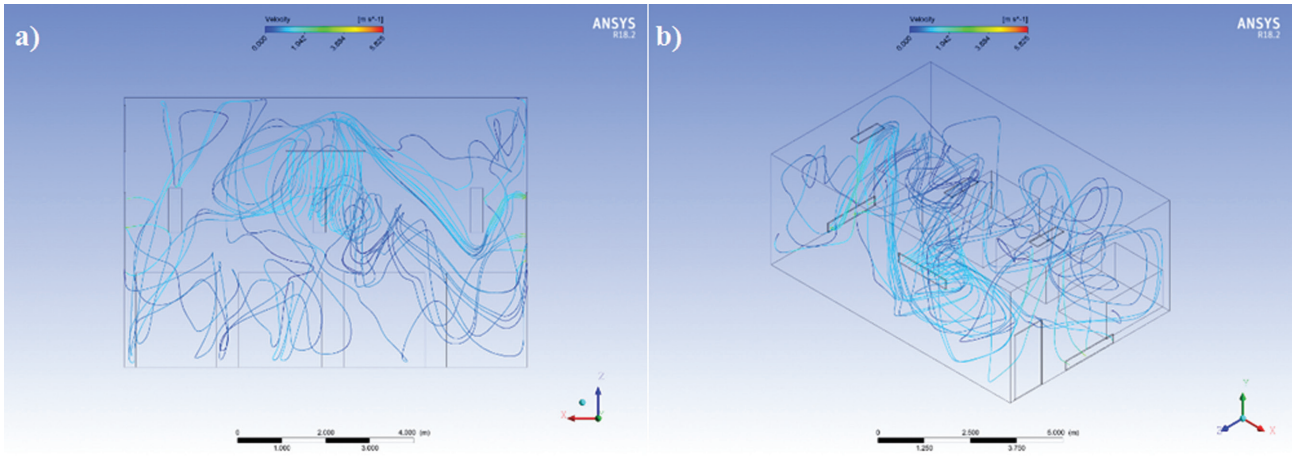

Figure 5. Distribution of streamlines start from sanitized air ventilation. (a) top view (XZ plane), (b) 3D view (XYZ plane).

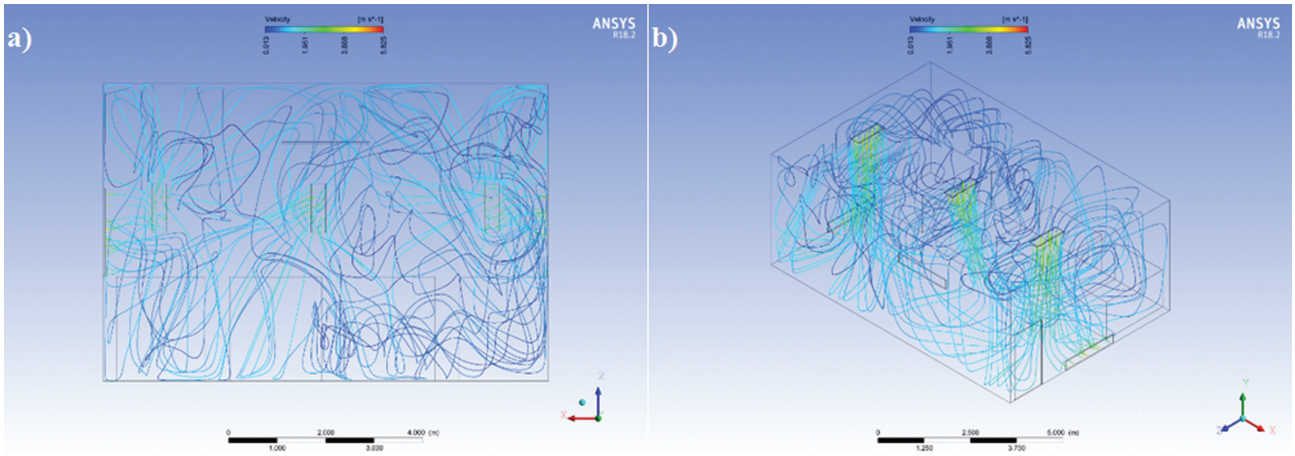

Figure 6. Distribution of streamlines initiated from air ventilation. (a) top view (XZ plane), (b) 3D view (XYZ plane).

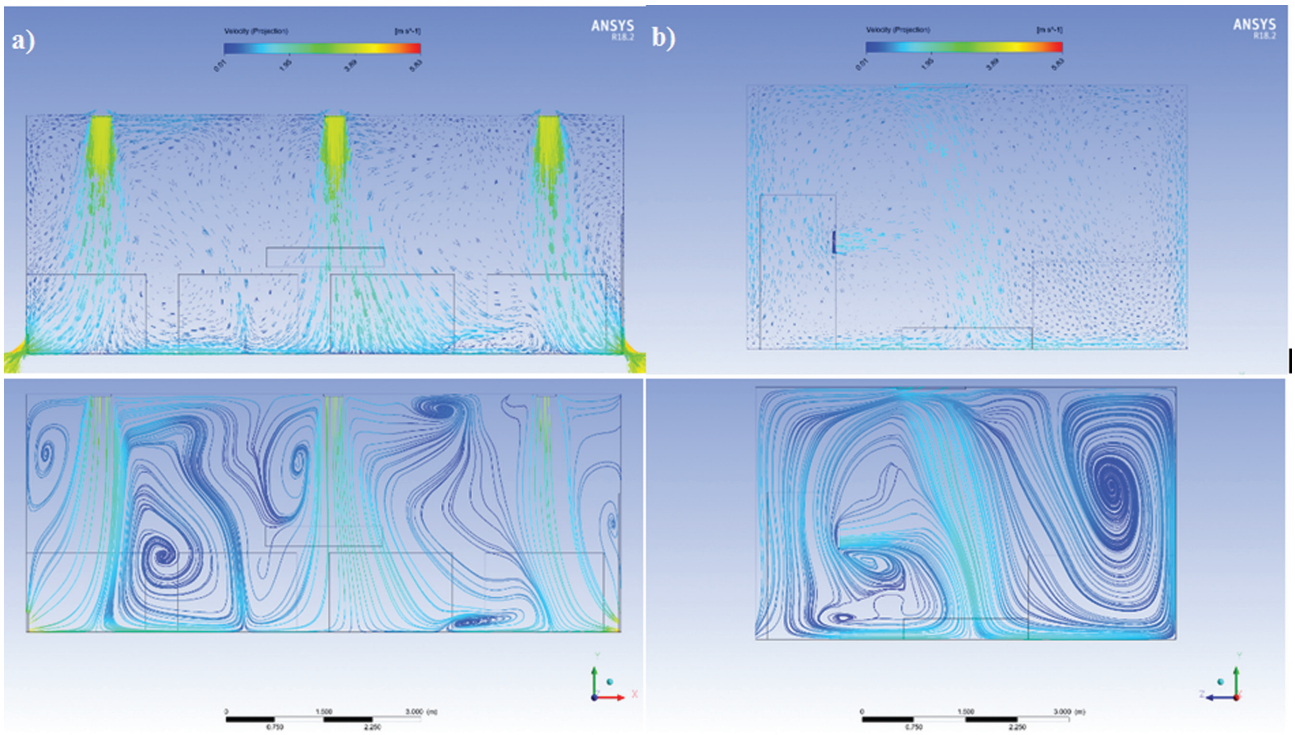

Figure 7. Air velocity distribution in an isolation room (Sanitized air machine and ventilation work at the same time). (a) XY plane, (b) YZ plane.

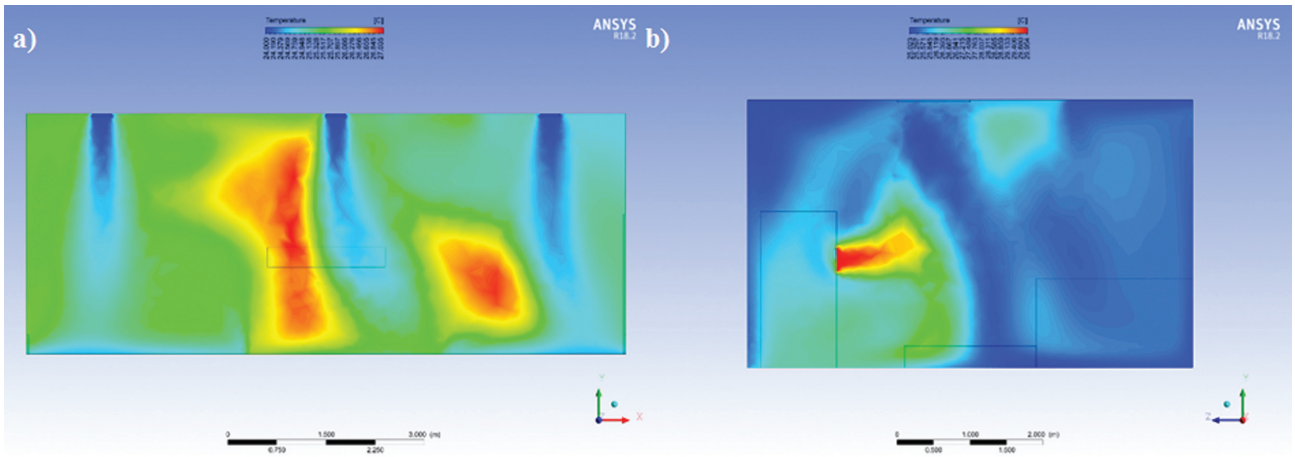

Figure 8. Temprature contour distribution in an isolation room (Sanitized air machine and ventilation work at the same time). (a) XY plane, (b) YZ plane.

CONCLUSIONS

This study was carried out to understand the flow physics of the air in the isolation room. In the study, it was carried out to investigate the conditioned air from the ventilation and sanitized air machine reaches every point of the room and the evacuation of the COVID-19 virus. For this, CFD analysis was performed and the standard k-epsilon model was chosen to perform numerical modelling. Considering that there is no known cure for the COVID-19 virus, it is necessary to minimize the risk of contracting the disease. This study has a crucial role at this point, because it is important to understand the physics of the fluid in the room to minimize the risk of getting the virus for patients and healthcare workers in the isolation room. As result of the flow modelling that was analyzed as unsteady in the study, it was concluded that it would be

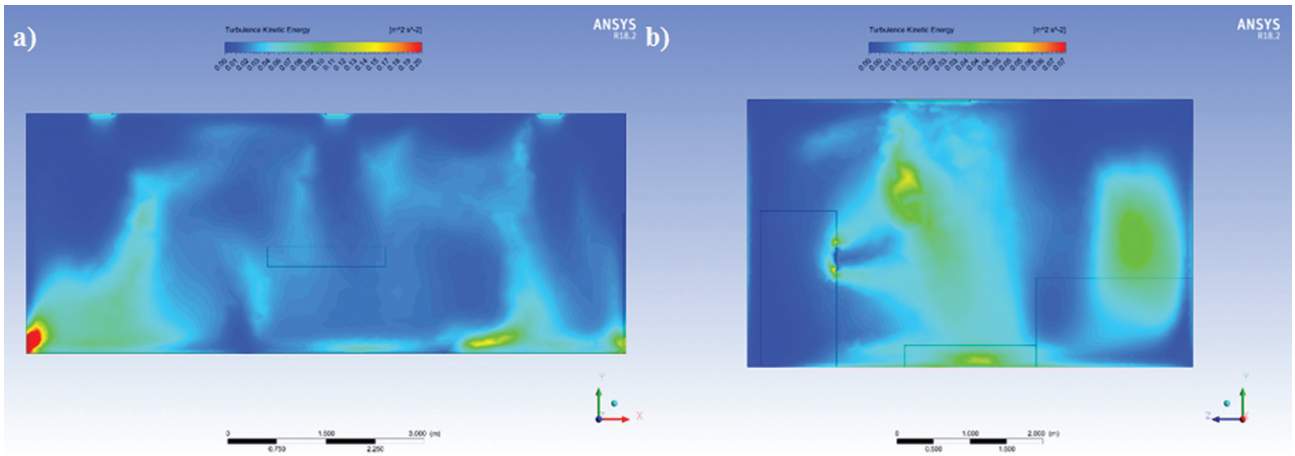

Figure 9. Turbulent kinetic energy contour distribution in isolation room (Sanitized air machine ventilation work at the same time). (a) XY plane, (b) YZ plane.

more possible to evacuate the COVID-19 virus by increasing the turbulence according to the volume of the isolation room.

- In this study, the situations causing the death of the virus because of the mixing of the air coming from the sterilized air machine and the ventilation in the isolation room were investigated.
- The presence of eddies in the room was revealed.
- The results of the study were compared with the previous experimental study and were found to be consistent.
- The k-epsilon model, which includes the equations of motion, was used in CFD analysis.
- From simulation analysis, it was found that high turbulent areas in the isolation chamber can be an effective way to disperse the disinfectant into a volume of the closed isolation chamber to kill or minimize the COVID-19 virus.

AUTHORSHIP CONTRIBUTIONS

Authors equally contributed to this work.

DATA AVAILABILITY STATEMENT

The authors confirm that the data that supports the findings of this study are available within the article. Raw data that support the finding of this study are available from the corresponding author, upon reasonable request.

CONFLICT OF INTEREST

The author declared no potential conflicts of interest with respect to the research, authorship, and/or publication of this article.

ETHICS

There are no ethical issues with the publication of this manuscript.

REFERENCES

[1] Salgotra R, Gandomi M, Gandomi AH. Evolutionary modelling of the COVID-19 pandemic in fifteen most affected countries. Chaos Solitons Fract 2020;140:110118. [CrossRef]

[2] Huang C, Wang Y, Li X, Ren L, Zhao J, Hu Y, et al. Clinical features of patients infected with 2019 novel coronavirus in Wuhan, China. Lancet 2020;395:497–506. [CrossRef]

[3] Lurie N, Saville M, Hatchett R, Halton J. Developing covid-19 vaccines at pandemic speed. N Engl J Med 2020;382:1969–1973. [CrossRef]

[4] Peng PWH, Ho PL, Hota SS. Outbreak of a new coronavirus: what anaesthetists should know. Br J Anaesthesia 2020;124:497–501. [CrossRef]

[5] Shi P, Dong Y, Yan H, Zhao C, Li X, Liu W, et al. Impact of temperature on the dynamics of the COVID-19 outbreak in China. Sci Total Environ 2020;728:138890. [CrossRef]

[6] World Health Organization. Modes of transmission of virus causing COVID-19: implications for IPC precaution recommendations: scientific brief, 29 March 2020. World Health Organization; 2020.

[7] Setti L, Passarini F, De Gennaro G, Barbieri P, Perrone MG, Piazzalunga A, et al. The potential role of particulate matter in the spreading of COVID-19 in Northern Italy: first evidence-based research hypotheses. MedRxiv. 2020. [CrossRef]

[8] Xie J, Zhu Y. Association between ambient temperature and COVID-19 infection in 122 cities

from China. Sci Total Environ 2020;724:138201. [CrossRef]
[9] Guo ZD, Wang ZY, Zhang SF, Li X, Li L, Li C, et al. Aerosol and surface distribution of severe acute respiratory syndrome coronavirus 2 in hospital wards, Wuhan, China, 2020. Emerging infectious diseases. 2020;26:1586. [CrossRef]
[10] Qian H, Li Y. Removal of exhaled particles by ventilation and deposition in a multibed airborne infection isolation room. Indoor Air 2010;20:284–297. [CrossRef]
[11] Cai J, Sun W, Huang J, Gamber M, Wu J, He G. Indirect virus transmission in cluster of COVID-19 cases, Wenzhou, China, 2020. Emerg Infect Dis 2020;26:1343. [CrossRef]
[12] Brumett AL. Indoor air treatment system with HEPA filtration. Accessed on Sep 16, 2003. Available at: https://www.freepatentsonline.com/y2003/0177777.html
[13] Gagnon D, Gagnon W, Eckhardt R. Sanitizing hand dryer. Accessed on Feb 4, 2020.
[14] Garcia KV, Garcia CP. Disinfecting device utilizing ultraviolet radiation with heat dissipation system. Accessed on Nov 4, 2008. Available at: https://patents.google.com/patent/US7444711B2/en
[15] Morawska L, Tang JW, Bahnfleth W, Bluyssen PM, Boerstra A, Buonanno G, et al. How can airborne transmission of COVID-19 indoors be minimised? Environ Int 2020;142:105832. [CrossRef]
[16] Razzini K, Castrica M, Menchetti L, Maggi L, Negroni L, Orfeo NV, et al. SARS-CoV-2 RNA detection in the air and on surfaces in the COVID-19 ward of a hospital in Milan, Italy. Sci Total Environ 2020;742:140540. [CrossRef]
[17] Zhou L, Wu S, Zhou M, Li F. 'School's out, but class' on', the largest online education in the world today: Taking China's practical exploration during The COVID-19 epidemic prevention and control as an example. Best Evid Chin Edu 2020;4:501–519. [CrossRef]
[18] Li Y, Leung GM, Tang J, Yang X, Chao C, Lin JZ, et al. Role of ventilation in airborne transmission of infectious agents in the built environment-a multidisciplinary systematic review. Indoor Air 2007;17:2–18. [CrossRef]
[19] Bhattacharyya S, Dey K, Paul AR, Biswas R. A novel CFD analysis to minimize the spread of COVID-19 virus in hospital isolation room. Chaos Solitons Fract 2020;139:110294. [CrossRef]
[20] Asgari S, Moazamigoodarzi H, Tsai PJ, Pal S, Zheng R, Badawy G, et al. Hybrid surrogate model for online temperature and pressure predictions in data centers. Future Generation Comput Syst 2021;114:531–547. [CrossRef]
[21] Kanaan M. CFD optimization of return air ratio and use of upper room UVGI in combined HVAC and heat recovery system. Case Stud Therm Eng 2019;15:100535. [CrossRef]
[22] Pichurov G, Stankov P, Markov D. Hvac control based on CFD analysis of room airflow. IFAC Proceed Volumes 2006;39:213–218. [CrossRef]
[23] Cao F, Zhang L, Pina A, Ferrão P, Fournier J, Lacarrière B, et al. Study of transient indoor temperature for a HVAC room using a and room Cooling using a Study of transient indoor temperature for a Heating HVAC modified CFD method. Energy Proced 2019;160:420–427. [CrossRef]
[24] Blom I, Itard L, Meijer A. Environmental impact of building-related and user-related energy consumption in dwellings. Build Environ 2011;46:1657–1669. [CrossRef]
[25] Arslan E, Aktaş M, Can ÖF. Experimental and numerical investigation of a novel photovoltaic thermal (PV/T) collector with the energy and exergy analysis. J Clean Prod 2020;276:123255. [CrossRef]
[26] Wang M, Lin CH, Chen Q. Advanced turbulence models for predicting particle transport in enclosed environments. Build Environ 2012;47:40–49. [CrossRef]
[27] Yadav AS, Shrivastava V, Dwivedi MK, Shukla OP. 3-dimensional CFD simulation and correlation development for circular tube equipped with twisted tape. Mater Today Proceed 2021;47:2662–2668. [CrossRef]
[28] Chung KC, Hsu SP. Effect of ventilation pattern on room air and contaminant distribution. Build Environ 2001;36:989–998. [CrossRef]
[29] Khelifa A, Touafek K, Moussa HB, Tabet I. Modeling and detailed study of hybrid photovoltaic thermal (PV/T) solar collector. Sol Energy 2016;135:169–176. [CrossRef]
[30] Misha S, Abdullah AL, Tamaldin N, Rosli M, Sachit F. Simulation CFD and experimental investigation of PVT water system under natural Malaysian weather conditions. Energy Rep 2020;6:28–44. [CrossRef]
[31] Yadav AS, Shrivastava V, Sharma A, Dwivedi MK. Numerical simulation and CFD-based correlations for artificially roughened solar air heater. Mater Today Proceed 2021;47:2685–2693. [CrossRef]
[32] Vickers NJ. Animal communication: when i'm calling you, will you answer too? Curr Biol 2017;27:R713–R715. [CrossRef]
[33] CFX-Solver A. Theory Guide, Release ll. ANSYS Inc, Canonsburg, PA. 2006;
[34] Kumar D, Premachandran B. Effect of atmospheric wind on natural convection based solar air heaters. Int J Therm Sci 2019;138:263–275. [CrossRef]
[35] Hazami M, Riahi A, Mehdaoui F, Nouicer O, Farhat A. Energetic and exergetic performances analysis of

a PV/T (photovoltaic thermal) solar system tested and simulated under to Tunisian (North Africa) climatic conditions. Energy 2016;107:78–94. [CrossRef]

[36] Ansys I. ANSYS FLUENT theory guide. Canonsburg, Pa. 2011;794.

[37] Fluent A. Ansys fluent theory guide. Ansys Inc, USA. 2011;15317:724–746.

[38] Bhattacharyya S, Chattopadhyay H, Biswas R, Ewim DR, Huan Z. Influence of inlet turbulence intensity on transport phenomenon of modified diamond cylinder: a numerical study. Arabian J Sci Eng 2020;45:1051–1058. [CrossRef]